

ORIGINAL ARTICLE

Synthesis and Characterisation of Indium Tin Oxide Thin Films for Dye-Sensitised Solar Cells using Natural Fruit Extracts

M.S. Ramyashree¹, Kshitij Kumar¹, S. Shanmuga Priya^{1,*} and K. Sudhakar^{2,3}

¹Department of Chemical Engineering, Manipal Institute of Technology, Manipal Academy of Higher Education, Manipal-576104, Karnataka, India

²Faculty of Mechanical and Automotive Engineering Technology, Universiti Malaysia Pahang, Pekan, 26600, Pahang, Malaysia

³Energy Centre, Maulana Azad National Institute of Technology, Bhopal, 462003, India

ABSTRACT – The study focuses on the application of natural fruit extract of blackberry in dye-sensitised solar cells (DSSC) as a photosensitiser. The widespread availability of the fruits and juices, high concentration of anthocyanins in them ease of extraction of anthocyanin dyes from these commonly available fruits, enable them as a novel and inexpensive candidates for solar cell fabrication. Anthocyanins are naturally occurring biodegradable and non-toxic compounds that can be extracted with minimal environmental impact and provide environmentally benign alternatives for manufacturing dyes in DSSC synthesis. Indium tin oxide (ITO) thin films are synthesised using sol-gel and spin-coating techniques. ITO characteristics are determined by x-ray diffraction (XRD), scanning electron microscopy (SEM), and Fourier transforms infrared spectra (FTIR) measurements. To find the transmittance percentage in the visible region of thin films, atomic force microscope (AFM) and UV-Vis spectroscopy analyses were done. The nanocrystalline phase of the synthesised ITO films was confirmed through XRD. SEM was used to analyse the morphology of the synthesised ITO films. Cubic, columnar (edge length ~ 35-45 nm) and rod-shaped (~110 x 14) particles were observed. Narrow size distribution was observed for spherical particles in the range of ~13-15 nm. The FTIR analysis revealed the presence of carboxyl and hydroxide functional groups. The AFM analysis revealed the uniform spread of the synthesised dye, while the visible region absorbance and transmittance of the synthesised ITO films were confirmed through UV-vis spectroscopy. The thin films showed 83-86% of average transmittance. Finally, we fabricated a dye-sensitised solar cell with desired properties. The characterisation results confirmed that the synthesised material could be used in the DSSC application.

ARTICLE HISTORY

Received: 18th Feb 2021

Revised: 30th Nov 2021

Accepted: 8th Dec 2021

KEYWORDS

Indium Tin Oxide;

Sol-gel;

Natural fruit extract;

Dye-sensitised solar cells;

Blackberry

INTRODUCTION

The dye-sensitised solar cell (DSSC) is a third-generation photovoltaic (PV) that has a simple manufacturing method and the potential for cheap manufacturing costs [1]. Michael Gratzel and their team came up with the Gratzel Cell known as dye-sensitised solar cells that imitate the photosynthesis process by sensitising a semiconductor [2]. However, many photovoltaic cells assured solar energy conversion from sunlight to electricity in the past years. Lower conversion efficiency, long-term stability, and higher cost limit their practical implementation [3], [4]. Generally, the significant components of DSSCs are photo-electrodes, photosensitisers, electrolytes, and counter electrodes[5]. Photosensitisers play an essential role among these four significant components, as they are the origin of light-harvesting in DSSCs [6]. Figure 1 shows the schematic diagram of the DSSC.

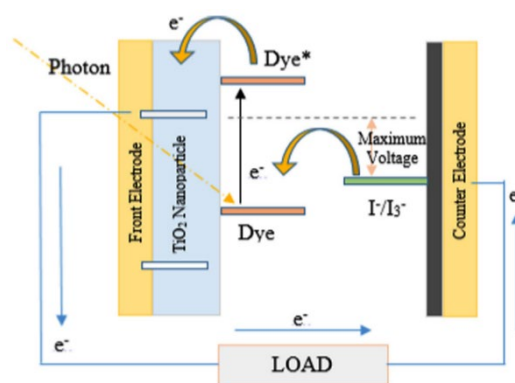


Figure 1. DSSC schematic band diagram [7].

Natural dyes are suitable for DSSCs devices due to their non-toxic, environmentally friendly, low cost, and abundance. Natural dyes, in particular, play an important role in green DSSCs [8]. Several natural pigments such as chlorophyll, anthocyanins, tannin, and carotene are successfully used as sensitizers in DSSC [9]. The sensitized dye works by absorbing the sunlight, later converted to electrical energy [2]. There are only a few characteristics that make a dye sensitizer effective. To begin, it must have a high absorption capacity in the visible range when illuminated by sunlight.

Furthermore, the dye molecules should have hydroxide or carboxyl groups that firmly graft to the TiO₂ surface's Titanium (IV) sites. It should also have the ability of efficient electron injection into the semiconductor's conduction band [10]. For photosensitization, anthocyanin is a pigment that imparts attractive red, blue, purple, and violet to berries and many other fruits and vegetables. Natural colours contain anthocyanins, a water-soluble pigment that absorbs light at the longest wavelength. Carbonyl and hydroxyl substituents in anthocyanin molecules serve as functional groups attached to the surface of a porous titanium dioxide substrate. The conduction band (CB) of metal oxides like TiO₂ receives the excited electrons [11].

Tahir et al. [12] synthesised DSSC using *Jatropha* and *Chrysanthemum*, which has purple pigment. The results showed that the dye absorbance was in the visible region. The mixture of both the extracts gave higher performance compared to the individual ones. Naresh Kumar et al. [9] extracted natural dye from *Terminalia Catappa* fruits. The cell efficiency was found to be 1.58% and confirmed its application for DSSC. Kenneth Obi et al. [1] choose *Opuntia Phaeacantha* and *Morus Rubra* natural colours to sensitise TiO₂ photoanodes in DSSCs. The raw prickly pear extract shows higher photovoltaic performance than any eluates, with a PV efficiency of 0.73%. Ammar et al. [4] extracted Chlorophyll and Anthocyanin from spinach, cabbage, and onion peels. The results showed that the DSSC based on chlorophyll dye performed best, with a power conversion efficiency of 0.17%.

TiO₂ has a more comprehensive application because of its non-toxicity, high thermal and chemical stability, low cost, and high transparency [13]. In addition to its application in DSSC, TiO₂ materials also have applications in electronics and photocatalysis. [14]. Indium tin oxide (ITO) is a conductive glass with low sheet resistance and high transmittance. ITO is an n-type wide bandgap semiconductor of around 4 eV and low resistivity. It possesses high transmittance in the visible region and excellent electrical conductivity [15]. The advantages of the sol-gel method are that it gives better control of structure, porosity, nanoparticles, better homogeneity, and less energy consumption. It finds application in smart windows [15], polymer-based electronics, and thin-film photovoltaics. ITO thin films can also serve as anti-reflective coatings and liquid crystal displays [16]. Thin-film deposition can be done using flame pyrolysis [17], CVD technique [18], electron deposition [19] and laser printing. [20], laser deposition [21] and sol-gel techniques [22]. The sol-gel method involves wet chemical processing to synthesise glassy or ceramic materials at low temperatures. It includes preparation and sol gelation, ultimately leading to liquid removal in the gel. Ammonia and sodium hydroxide find applications in indium and tin salts hydrolysis [26],[27].

Qiao et al. [23] prepared ITO thin films from screen printing method. The electrical properties of ITO film was improved by changing the mass ratio of cubic-shaped ITO nanoparticles to ethyl cellulose. Dong et al [24] synthesised ITO thin films using sol gel spin coating technique. ITO thin film was thermal treated at 250 °C showed remarkable conductivity. Dhamodharan et al [25] synthesised Al doped ZnO thin films onto ITO substrate for DSSC application. Transmittance of 85% was observed on the AZO film in the visible region. There was increase in electrical resistivity upon increase in the Al doping beyond 1.5%. The objective is to use ITO-coated glass substrate as a thin film material to synthesise DSSC using natural fruit extracts containing anthocyanin pigment and analyse the results.

EXPERIMENTAL

Preparation of Xerogel Powder

Indium chloride tetrahydrate, tin chloride pent hydrate, aqueous NH₃ solution, and ethanol were purchased from Aldrich, Germany. 1.17 grams of Indium chloride tetra-hydrate and 0.1402 g of Tin chloride pent-hydrate were put into 100 ml distilled water. Later, 2 ml aqueous ammonia solution was added to it at room temperature, and the mixture was stirred for 30 mins. It underwent ultrasonic treatment for 5 minutes. Then it was placed in a centrifuge at a speed of 5000 rpm for 30 minutes. After this, it is dispersed in 50 ml distilled water and undergoes dialysis for three days. Then, it underwent centrifugation at 12000 rpm for 30 minutes. Subsequently, it underwent washing with 50 ml of absolute ethanol. The sediment was washed and centrifuged again and again 3-4 times to remove the unwanted chloride ions from it. Finally, the sediment was dispersed in absolute ethanol and underwent an ultrasonic water bath. Ethanol was evaporated from the ITH sol at 80 °C to obtain ITH xerogel powder. Figure 2 shows the schematic flow diagram of the procedure.

Synthesis of ITO Powders and Thin Films

The obtained ITH xerogel powder was calcinated at 550 °C to obtain ITO powders. The ITH thin film was deposited onto the substrates by spin-coater. 45 µl of xerogel was dropped over the soda-lime substrate rotating at 3000 rpm and subsequently dried inside the spin coater for the 30 s. The deposited layer was calcined at 550 °C for 30 min in the air to obtain ITO thin films. FTIR measurements were made with 25 samples at a 4 cm⁻¹ using the SHIMADZU IR Spirit-T model and Rigaku Miniflex 600 (5th generation) with an operating voltage of 40 kV, and a current flow of 15 mA did the XRD analysis. EVO MA18 with Oxford EDS(X-act) operated at 10 kV did the SEM analysis, and SHIMADZU UV-3600 Plus did the UV-Vis spectroscopy analysis. The efficiency of the solar cell is one of the critical parameters of the solar cell. To calculate the efficiency, Eq. (1) and Eq. (2) were used.

$$P_{max} = V_{oc} * I_{sc} * FF \quad (1)$$

$$\eta = \frac{V_{oc} * I_{sc} * FF}{P_{in}} \quad (2)$$

Where, V_{oc} is open-circuit voltage (V), I_{sc} is short-circuit current (A), FF = fill factor, η is efficiency (%), P is maximum power output, and power input (W). The open-circuit voltage and short-circuit current are the maximum voltage and current that the solar cell can handle. At both of these operating points, there is still no power. The fill factor (FF) stands for the parameter which, in conjunction with V_{oc} and I_{sc} , determines the maximum power output of the solar cell. The definition of the FF is the ratio of maximum power from the solar cell to the product of V_{oc} and I_{sc} . All these parameters can only be measured when the cell is fully operating.

Two grams of blackberry fruits are mixed into 12 ml of 95% ethanol and 12 ml of 15% acetic acid at room temperature separately. The fruits were mashed using mortar and pestle. ITO coated glass substrate was taken as a photoanode with a conductive coating on it. The conductive side of the ITO substrate was measured using a multimeter, as shown in Figure 3.

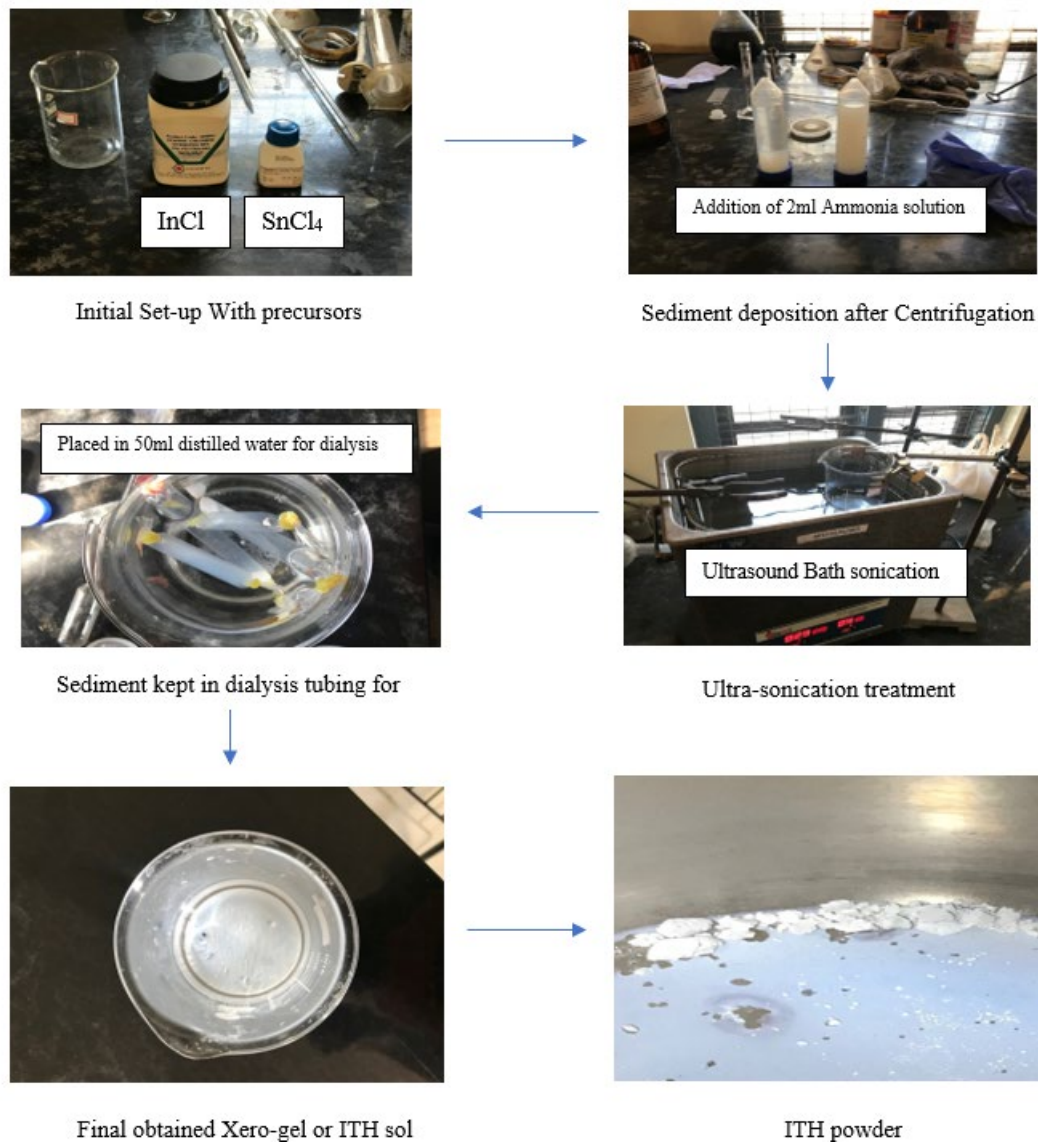


Figure 2. Synthesis of ITH sol.

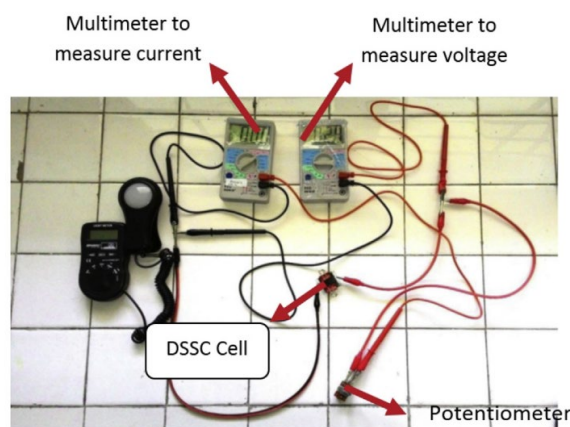


Figure 3. Measurement of I-V curve on DSSC [26].

Preparation of Photoanode

The photoanode (working electrode) was prepared by adsorbing the dye (extracted from natural fruit extracts using mortar and pestle in a beaker) on the porous titanium dioxide TiO_2 layer, deposited on ITO conducting glass. About 2-3 drops of the dye were poured on the TiO_2 coated ITO glass substrate.

Preparation of Counter Electrode and Electrolyte

After checking for the ITO coated glass substrate's conductive side, the ITO glass was wiped with ethanol and deionised water to prepare the carbon counter electrode. Later the ITO glass surface was covered using graphite carbon pencil with a uniform graphite coating covering the glass. Graphite acts as the catalyst for the reaction.

In the electrolyte preparation, 10 ml of ethylene glycol and 0.127 grams of iodine were mixed in a beaker. 0.83 grams of potassium iodide was added and stirred well to the existing. Hence the redox mediator was used as the electrolyte. The iodide redox couple acted as the filler for the dye.

The glass slides were placed on top of each other to maintain offset. The cells were sealed using binder clips on the sides that were not overhanging. Two electrodes were connected across the cell, and voltage was measured using a voltmeter.

Optimisation and Characterisation of DSSC

Dyes extracted from natural fruit extracts containing light-harvesting pigments like anthocyanin pigments were used to fabricate DSSC. The synthesised ITO film was characterised using XRD, AFM, FTIR, SEM, and UV-visible spectroscopy to account for Morphology, crystallinity, uniform distribution, functional group, morphology, and transmittance. Hence, all suitable parameters like open circuit voltage and short circuit current can be obtained after optimising photoanode and counter electrode.

RESULTS AND DISCUSSION

Figure 4(a) and 4(b) show the XRD pattern of ITO powder and ITO thin film. In XRD pattern of the xerogel powder cubic $\text{In}(\text{OH})_3$. $\text{In}(\text{OH})_3$ was the dominant crystal phase. The graphs did not display any peaks which could reveal the presence of Sn, SnO , or SnO_2 , showing complete miscibility of In and Sn atoms in the In_2O_3 lattice. Sn has tetravalent valency. Hence, each Sn (IV) replaces In(III) substitutionally and donates free electrons for conductivity. The XRD patterns of all ITO films displayed crystalline structure matching In_2O_3 reference peaks from the literature [27]. In Figure 4(a), the XRD pattern did not contain any peaks, which meant that the thin film was amorphous. However, the ITO powder sample, which showed peaks, revealed its nanocrystalline structure [28]. The precipitate was for three days which favoured the formation of nanocrystalline ITH. The peak between 20 and 30 degree is due to the impurity present in the synthesised ITO thin films.

SEM analysis was carried out on the ITO nanoparticles to account for their roughness and smoothness. Polyhedral and spherical shapes were observed for the nanoparticles at 3 μm (in Figure. 5(a) and 5(b)) and 10 μm (in Figure 5(c) and Figure 5(d)). Cubic, columnar (edge length $\sim 35\text{-}45$ nm) and rod-shaped ($\sim 110 \times 14$) particles were reported. Narrow size distribution was observed for spherical particles within the range of $\sim 13\text{-}15$ nm. The above SEM pictures reported a porous structure. The fine particles were mostly round-shaped.

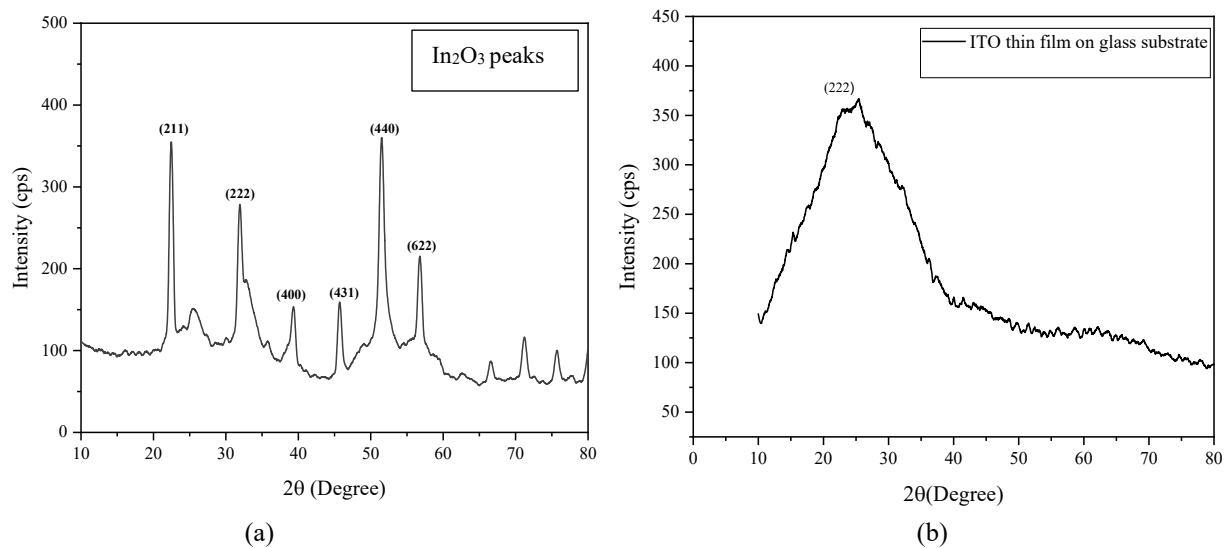


Figure 4. XRD pattern of (a) ITO nanoparticles and (b) ITO thin film on a glass substrate.

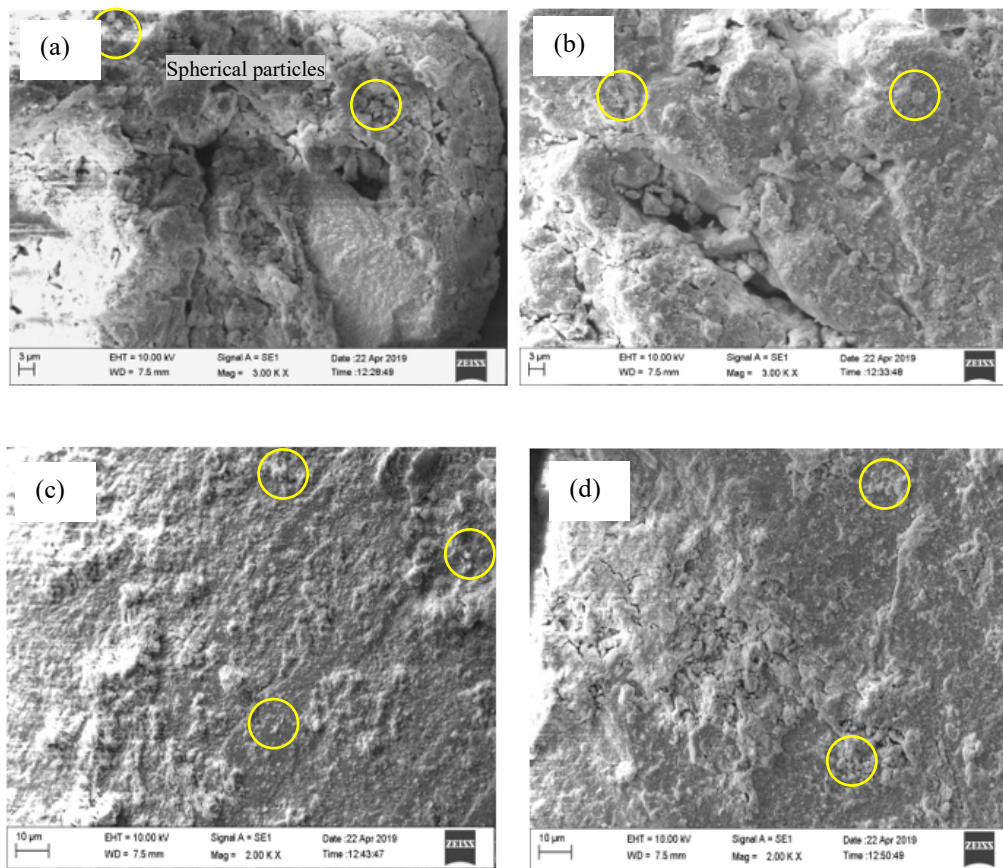


Figure 5. SEM image of (a), (b) ITO nanoparticle at 3 μm (c), (d) ITO nanoparticle at 10 μm.

From Figure 6, we can analyse the FTIR spectra of the nanoparticles synthesised by the sol-gel over the range of 500 cm^{-1} to 4000 cm^{-1} . The vibration modes show the presence of OH at 3230.77 cm^{-1} to 3248 cm^{-1} and 839.03 cm^{-1} to 983.70 cm^{-1} . The band at 1157.29 cm^{-1} shows the terminal hydroxyl group of In(OH) and the hydroxyl group of Sn(OH), which means that some hydroxyl groups were not converted into oxide members. The band from 414.70 cm^{-1} to 507.28 cm^{-1} relates In-O-In.

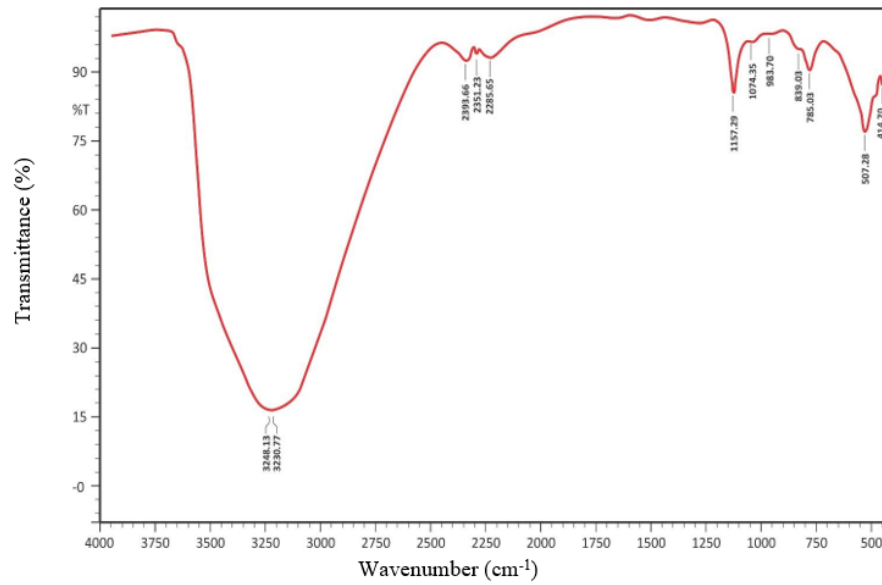


Figure 6. FTIR spectra of ITO nanoparticles.

Figure 7 shows the characteristics of surface composition and structural morphology from AFM under normal temperature conditions. Characteristics of surface composition and structural morphology were studied from AFM under normal temperature conditions. The microscope was operated in contact mode, and scans were obtained at various points on the film surface. AFM images of ITO thin films were collected overscan areas of (1×1) , $(3 \times 3) \mu\text{m}^2$. The height of AFM data points (scale z) was changed to ASCII data. Figure 7(a) to 7(d) show the ITO thin films possessing a continuous island structure. The average roughness was 25.98 nm for the scan area of $(1 \times 1) \mu\text{m}^2$ and its corresponding RMS value was 34.2 nm. The skewness factor was less than 2. The synthesised ITO got uniformly distributed on the surface.

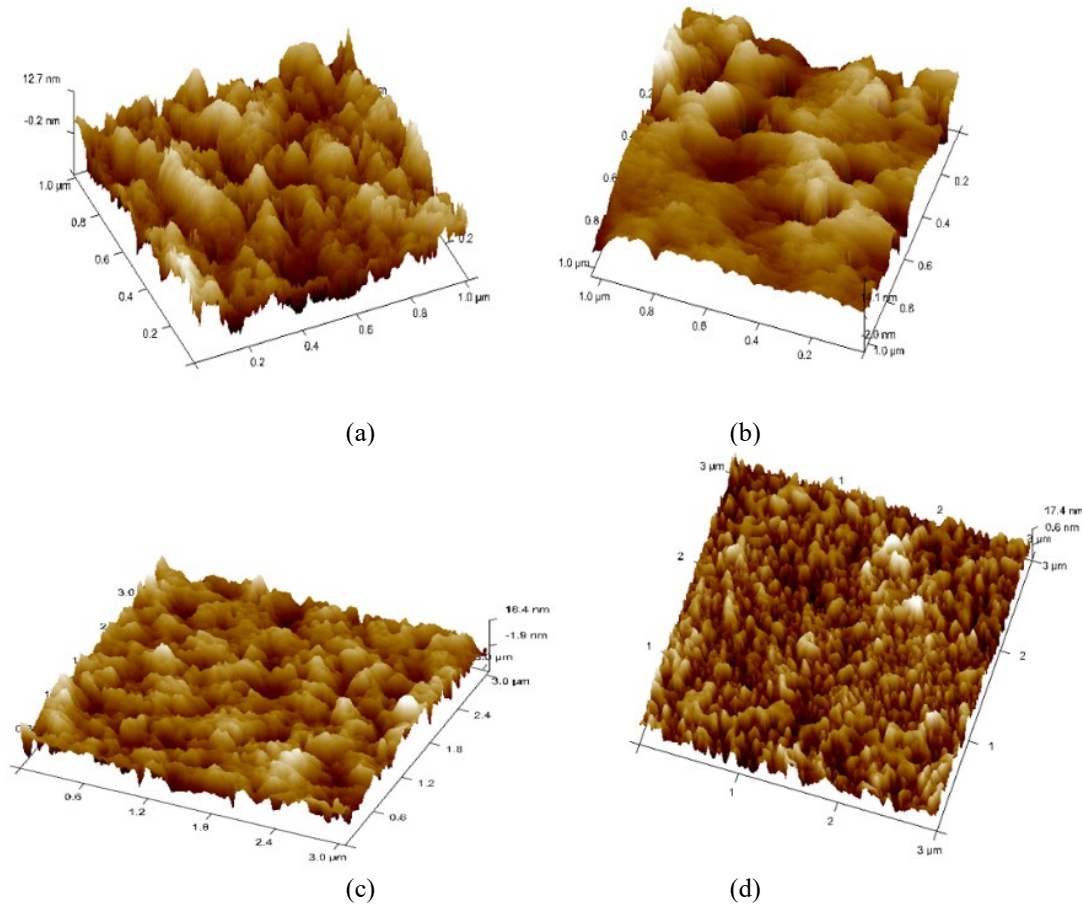


Figure 7. (a) AFM image of ITO thin film at $(1 \times 1) \mu\text{m}^2$ (b) ITO thin film AFM image from a different angle $(1 \times 1) \mu\text{m}^2$ (c) AFM image at $(3 \times 3) \mu\text{m}^2$ (d) AFM image at $(3 \times 3) \mu\text{m}^2$

Figures 8(a) and 8(b) show the transmission and absorbance spectra of ITO thin films. The wavelength corresponding to the measurement was in the range of 300-800 nm, and 83-86 % was the average transmittance. Xia et al. [29] reported that 92.66% transmittance ranges from 400-700 nm. Thirumoorthi et al. [30] reported the average transmittance rate of 82-87% for tin-doped films. Hence the results confirm that the synthesised material is active in the visible region and has potential application in DSSC as a photosensitiser.

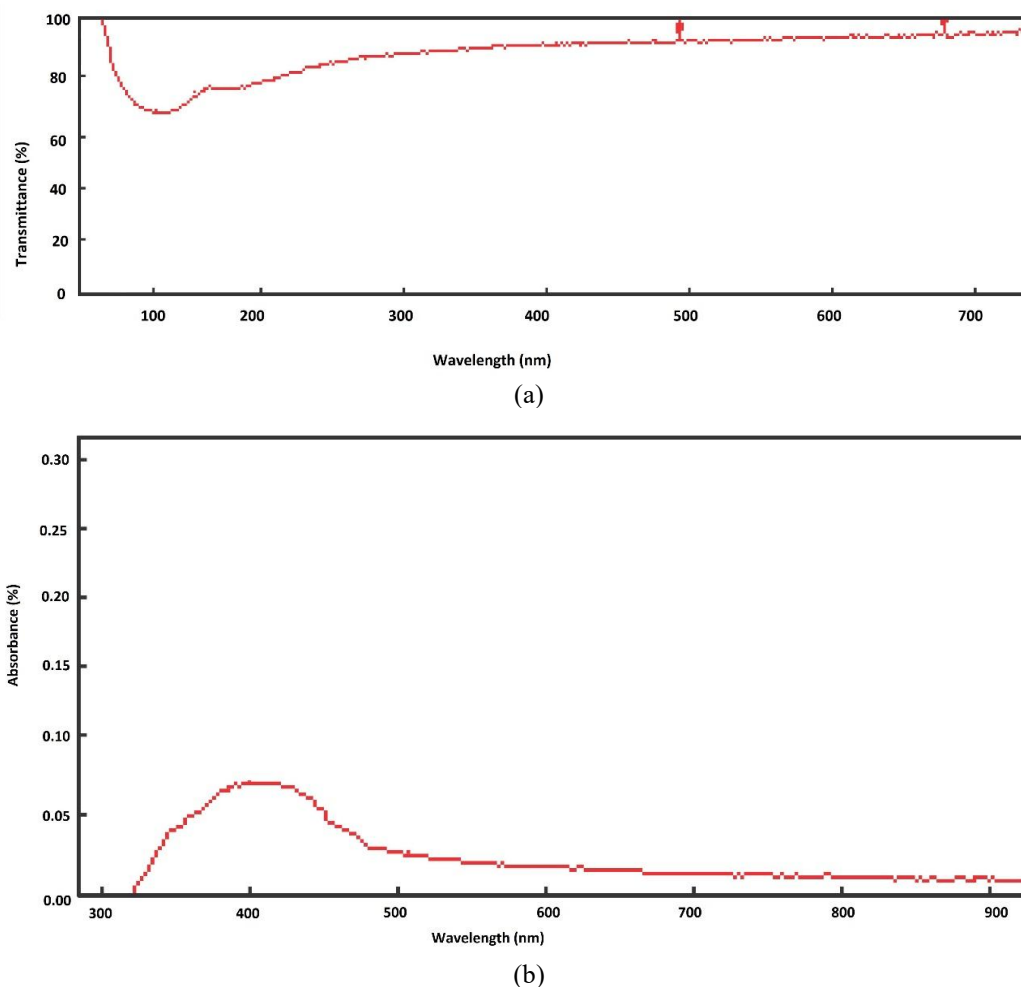


Figure 8. UV-Vis (a) transmission spectra and (b) UV-Vis absorbance spectra of ITO thin film.

CONCLUSION

In this work, ITO thin films were synthesised from sol-gel spin-coating techniques using natural plant extract, and the properties of ITO films were studied. On careful analysis of the results, we can conclude that ITO is well suited for solar cell applications because of its enhanced transparent nature in the visible region. The natural dyes extracted showed good characteristics as a photosensitiser, which includes visible light absorption and anchoring groups such as hydroxyl and carbonyl functional groups. The XRD analysis confirmed the crystallinity of ITO thin films. AFM analysis confirmed the uniform spread of the natural. Hence, the results show the potential of the synthesised natural plant extract in DSSC application.

ACKNOWLEDGEMENT

The authors would like to acknowledge the Department of Chemical Engineering, Manipal Institute of Technology, Manipal Academy of Higher Education, Manipal for their support. The authors would like to acknowledge Central Instrumental Facility, Manipal Institute of Technology, Manipal Academy of Higher Education for their support in characterising XRD, SEM, and AFM. The authors also like to acknowledge the Manipal College of Pharmaceutical Science (MCOPS) for their support in the FTIR characterisation of the samples.

REFERENCES

- [1] K. Obi, L. Frolova, and P. Fuieler, "Preparation and performance of prickly pear (*Opuntia phaeacantha*) and mulberry (*Morus rubra*) dye-sensitised solar cells," *Sol. Energy*, vol. 208, no. July, pp. 312–320, 2020, doi: 10.1016/j.solener.2020.08.006.
- [2] M. Gratzel, "Synthesis and characterisation of dye sensitised solar cell," *Int. Res. J. Eng. Technol.*, vol. 4, no. 2, pp. 277–285, 2017.

- [3] O. Adedokun *et al.*, “Natural dye extracts from fruit peels as sensitiser in ZnO-based dye-sensitised solar cells,” *IOP Conf. Ser. Earth Environ. Sci.*, vol. 173, no. 1, 2018, doi: 10.1088/1755-1315/173/1/012040.
- [4] A. M. Ammar *et al.*, “Dye-Sensitised Solar Cells (DSSCs) based on extracted natural dyes,” *J. Nanomater.*, vol. 2019, 2019, doi: 10.1155/2019/1867271.
- [5] J. Ramirez-Perez, C. Maria, and C. P. Santacruz, “Impact of solvents on the extraction and purification of vegetable dyes onto the efficiency for dye-sensitised solar cells,” *Renewables Wind. Water, Sol.*, vol. 6, no. 1, pp. 1–15, 2019, doi: 10.1186/s40807-019-0055-x.
- [6] R. L. Vekariya *et al.*, “Humic acid as a sensitiser in highly stable dye solar cells: Energy from an abundant natural polymer soil component,” *ACS Omega*, vol. 1, no. 1, pp. 14–18, 2016, doi: 10.1021/acsomega.6b00010.
- [7] V. Sugathan, E. John, and K. Sudhakar, “Recent improvements in dye sensitised solar cells: A review,” *Renew. Sustain. Energy Rev.*, vol. 52, pp. 54–64, 2015, doi: 10.1016/j.rser.2015.07.076.
- [8] D. D. Babu *et al.*, “Highly efficient panchromatic dye-sensitised solar cells: Synergistic interaction of ruthenium sensitiser with novel co-sensitisers carrying different acceptor units,” *dye. Pigment.*, vol. 132, pp. 316–328, 2016.
- [9] P.N. Kumar and K. Sakthivel, “Terminalia catappa fruit pigments for dye sensitised solar cell applications,” *Journal of Advances in Chemistry*, vol. 12, no. 27, pp. 5809-5813, 2017.
- [10] M. C. Ung *et al.*, “Fruit based dye sensitised solar cells,” *IOP Conf. Ser. Mater. Sci. Eng.*, vol. 217, no. 1, 2017, doi: 10.1088/1757-899X/217/1/012003.
- [11] M. Hosseinnazhad and K. Gharanjig, “Investigation of green dye-sensitised solar cells based on natural dyes,” *Int. J. Chem. Mol. Eng.*, vol. 11, no. 6, pp. 464–467, 2017.
- [12] D. Tahir *et al.*, “Dye sensitised solar cell (DSSC) with natural dyes extracted from *Jatropha* leaves and purple *Chrysanthemum* flowers as sensitiser,” *J. Phys. Conf. Ser.*, vol. 979, no. 1, 2018, doi: 10.1088/1742-6596/979/1/012056.
- [13] S. Umale *et al.*, “Improved efficiency of DSSC using combustion synthesised TiO₂,” *Mater. Res. Bull.*, vol. 109, pp. 222–226, 2019, doi: 10.1016/j.materresbull.2018.09.044.
- [14] S. Nezar *et al.*, “Properties of TiO₂ thin films deposited by rf reactive magnetron sputtering on biased substrates,” *Appl. Surf. Sci.*, vol. 395, pp. 172–179, 2017, doi: 10.1016/j.apsusc.2016.08.125.
- [15] M. Cannistraro, M. E. Castelluccio, and D. Germanò, “New sol-gel deposition technique in the Smart-Windows – Computation of possible applications of Smart-Windows in buildings,” *J. Build. Eng.*, vol. 19, no. May, pp. 295–301, 2018, doi: 10.1016/j.jobe.2018.05.018.
- [16] Y. Sung *et al.*, “Anti-reflective coating with a conductive indium tin oxide layer on flexible glass substrates,” *Appl. Opt.*, vol. 57, no. 9, p. 2202, 2018, doi: 10.1364/ao.57.002202.
- [17] S. Saravanan, K. Ranganathan, and V. Jayaram, “Deposition and characterisation of oxide thin films by combustion spray pyrolysis,” in *Handbook of Modern Coatings Technologies* (Vol I), A. Ali, C. Laidani, and De Hosson, Eds., Elsevier 2016, pp. 139-179.
- [18] H. Pedersen, S. T. Barry, and J. Sundqvist, “Green CVD—Toward a sustainable philosophy for thin film deposition by chemical vapor deposition,” *J. Vac. Sci. Technol. A*, vol. 39, no. 5, p. 051001, 2021, doi: 10.1116/6.0001125.
- [19] K. O. Ukoba, A. C. Eloka-Eboka, and F. L. Inambao, “Review of nanostructured NiO thin film deposition using the spray pyrolysis technique,” *Renew. Sustain. Energy Rev.*, vol. 82, pp. 2900–2915, 2018, doi: <https://doi.org/10.1016/j.rser.2017.10.041>.
- [20] P. J. Diemer *et al.*, “Laser-printed organic thin-film transistors,” *Adv. Mater. Technol.*, vol. 2, no. 11, pp. 1700167, 2017, doi: <https://doi.org/10.1002/admt.201700167>.
- [21] M. Fenech and N. Sharma, “Pulsed laser deposition-based thin film microbatteries,” *Chem. – An Asian J.*, vol. 15, no. 12, pp. 1829–1847, 2020, doi: <https://doi.org/10.1002/asia.202000384>.
- [22] H. Kwon *et al.*, “Printable ultra-flexible fluorinated organic–inorganic nanohybrid sol–gel derived gate dielectrics for highly stable organic thin-film transistors and other practical applications,” *Adv. Funct. Mater.*, vol. 31, no. 10, p. 2009539, 2021, doi: <https://doi.org/10.1002/adfm.202009539>.
- [23] F. Qiao *et al.*, “A combined experimental and theoretical study of screen-printing high transparent conductive mesoscopic ITO films,” *Sci. Rep.*, vol. 10, no. 1, p. 5024, 2020, doi: 10.1038/s41598-020-61124-w.
- [24] L. Dong *et al.*, “Preparation of indium tin oxide (ITO) thin film with (400) preferred orientation by sol–gel spin coating method,” *J. Mater. Sci. Mater. Electron.*, vol. 30, no. 8, pp. 8047–8054, 2019, doi: 10.1007/s10854-019-01126-1.
- [25] P. Dhamodharan *et al.*, “Al-doped ZnO thin films grown onto ITO substrates as photoanode in dye sensitised solar cell,” *Sol. Energy*, vol. 141, pp. 127–144, 2017, doi: <https://doi.org/10.1016/j.solener.2016.11.029>.
- [26] H. Setyawati *et al.*, “Effect of metal ion Fe(III) on the performance of chlorophyll as photosensitisers on dye sensitised solar cell,” *Results Phys.*, vol. 7, pp. 2907–2918, 2017, doi: 10.1016/j.rinp.2017.08.009.
- [27] D. Chakraborty *et al.*, “XRD, UV-Vis-NIR and FT-IR Studies of ITO and Cr : ITO thin films prepared by electron beam evaporation technique,” *Mechanics, Materials Science & Engineering*, December 2017, 2018, doi: 10.2412/mmse.36.15.807ff.fhal-01966349f.
- [28] M. Thirumoorthi and J. Thomas Joseph Prakash, “Structure, optical and electrical properties of indium tin oxide ultra thin films prepared by jet nebuliser spray pyrolysis technique,” *J. Asian Ceram. Soc.*, vol. 4, no. 1, pp. 124–132, 2016, doi: 10.1016/j.jascer.2016.01.001.
- [29] N. Xia and R. A. Gerhardt, “Fabrication and characterisation of highly transparent and conductive indium tin oxide films made with different solution-based methods,” *Mater. Res. Express*, vol. 3, no. 11, pp. 0–23, 2016, doi: 10.1088/2053-1591/3/11/116408.
- [30] M. Thirumoorthi and J. Thomas Joseph Prakash, “Structure, optical and electrical properties of indium tin oxide ultra thin films prepared by jet nebuliser spray pyrolysis technique,” *J. Asian Ceram. Soc.*, vol. 4, no. 1, pp. 124–132, 2016, doi: <https://doi.org/10.1016/j.jascer.2016.01.001>.